Image Synthesis of Small Semiconductor Gamma Camera and Optical Camera for Identifying Sentinel Lymph Nodes in Radioguided Surgery

Hideaki Haneishi, Yoshimi Onishi and Hideki Hayashi

Abstract-- **We have developed a method that combines a small semiconductor gamma camera with an optical camera to synthesize the two kinds of images and help surgeons to easily identify sentinel lymph nodes on the gastric surface in the cancer resection surgery. The proposed method includes some key techniques such as distortion correction of the optical camera image, distance estimation between the camera head and the object surface using a laser and the optical camera, and perspective transformation of the gamma camera image to fuse with the optical camera image. The method and preliminary experimental results with a prototype setup are presented.**

I. Introduction

For gastric cancers, extensive lymphadenectomy has been performed as a standard surgical intervention. But it is important to avoid excessive lymphadenectomy when considering postoperative quality of life of patients. On the other hand, it is strongly supported by many studies that the sentinel lymph node (SN) represents the first lymph node to receive drainage from the primary tumor and therefore the absence of metastases in SNs supposedly correlates to no metastasis in downstream lymph nodes. So a minimally invasive technique that could diagnose the status of regional lymph nodes would allow lymphadenectomy to be avoided in patients without involved nodes. In those patients, resection of the primary tumor should be sufficient. In this trend, the feasibility and accuracy of SN biopsy to predict the status of non-SN lymph nodes have been evaluated in gastric cancers. Those evaluation studies showed favorable results using a single tracer, 99mTc-Tin colloid, to detect SNs [1].

Actual procedure of the radioguided stomach surgery is as follows. The tracer is injected onto the stomach inner surface around the primary tumor using an endoscope on a day before the operation. In the operation, surgeons open the patient's abdomen and make the gastric outer surface appeared. Radioactive lymph nodes are found by any gamma ray detection technique and the biopsy of those tissues is carried out. Based on the presence/absence of metastases in SNs, the area of resection is determined and resection surgery is performed.

Manuscript received November 13, 2005.
Hideaki Haneishi is with the Research Center for Frontier Medical Engineering, Chiba University, Chiba, 263-8522, Japan. He is also with Graduate School of Science and Technology, Chiba University, Chiba, 263-8522, Japan (e-mail: haneishi@faculty.chiba-u.jp).
Yoshimi Onishi is with Graduate School of Science and Technology, Chiba University. Hideki Hayashi is with the Research Center for Frontier Medical Engineering, Chiba University.

For observation of the radioactive distribution, gamma probes have been used. However, the probe shows only by sound if there is a radioactive source around the probe. An operator had to search a wide area of gastric surface. It was a time-consuming, less-quantitative and troublesome operation. Recently, a small semiconductor gamma camera (abbreviated to GC in this paper) has been available [2]. Since this camera is small enough and allows two dimensional imaging of the tracer distribution, the use of this camera instead of conventional gamma probes in radioguided gastric surgery is promising. In fact, fundamental experiments using animals have been performed already. However, there is a new problem that it is difficult to relate the output image of the GC to the real gastric surface. After collecting gamma rays from the gastric surface, surgeons remove the camera and try to make sure which part on the real gastric surface the radioactive area corresponds to. After removing the camera, however, it is often difficult.

For this issue, we have developed a method that combines a GC with an optical camera (abbreviated to OC). It is expected that by imaging the target area with GC and OC and synthesizing them, surgeons easily identify the SNs on the real surface. The method and preliminary experimental results with a prototype system are presented.

II. Method

A. *Outline of the method*

In the first setup, we decided to attach a small CCD camera with a wide-angle lens at the edge of the GC head. The schematic illustration of the setup is shown in Fig. 1. Normally, an image of the GC is captured at the distance of 3-10cm from the target surface. The obtained two-dimensional GC image represents the radioactivity distribution integrated along the direction of the collimator of the GC. In fact, in the case that the tracer is injected into the primary tumor, the tracer distribution is limited near the gastric surface. We also approximate the stomach wall of interest with the tracer distribution by a plane parallel to the head surface of the GC. Under this assumption, the position of the radioactivity distribution doesn't change by the distance between the GC camera head and the object surface though the resolution itself changes.

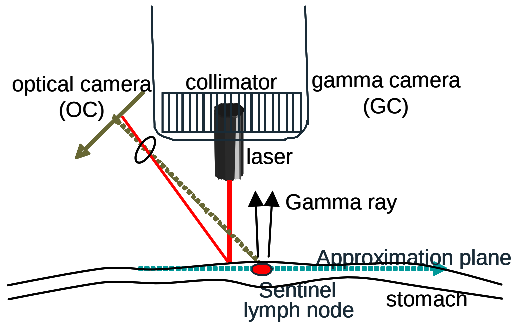

Fig. 1 Schematic illustration of the prototype setup for obtaining the gamma camera image and the optical camera image.

On the other hand, in the OC imaging, the radiance distribution of the visible light on the gastric surface is perspective-projected onto the image plane. Furthermore, the image is heavily distorted due to the wide-angle lens. This distortion must be corrected first. A correction method that we have developed before is one choice [3]. After the distortion correction, the pinhole camera model can be used to represent the mapping from the object space to image plane.

The image by this projection, in turn, depends on the distance between the GC camera head and the object surface. We, therefore measure the distance using a laser and the optical camera. Once the distance is obtained, the GC image approximated as the radioactivity distribution on the approximation plane is perspective-projected onto the OC image plane and synthesized with the OC image. The processing flow mentioned above is illustrated in Fig. 2.

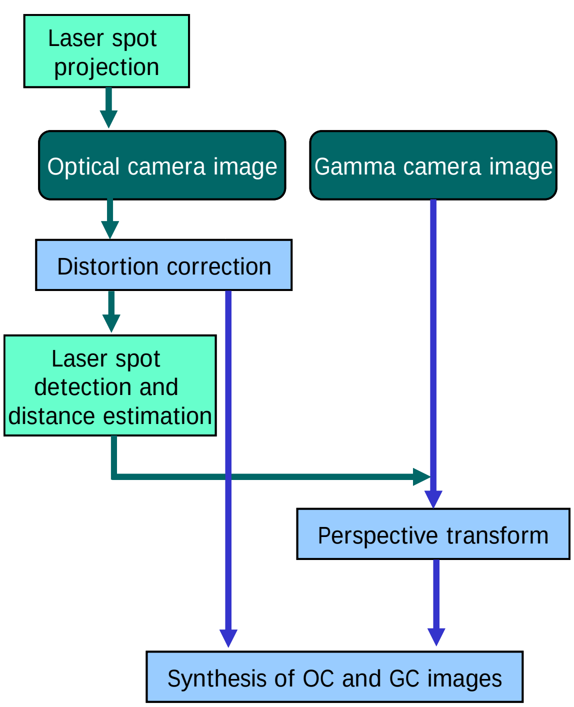

Fig. 2 Processing flow to obtain synthesized images.

B. Detail of image registration and synthesis technique

At first, the coordinates of the GC and OC imaging are defined as figure 3. Here, the object space related to the GC is defined as (*X*,*Y*,*Z*), and that related to the OC is defined as (*U*,*V*,*W*). The GC image coordinates are also defined by (*x*,*y*) where x is the same as *X* and *y* is the same as *Y*. Similarly, the optical camera image coordinates are defined by (*u*,*v*) where *u* is the same as *U* and *v* is the same as *V*. In the followings, we describe first how to relate the GC image coordinates (*x*,*y*) to the OC image coordinates (*u*,*v*) then, how to estimate the distance between the camera head to the object surface from the laser spot on the OC image.

In the imaging by the OC, The relationship between an object point (*U*,*V*,*W*) and its image coordinate (*u*,*v*) can be expressed by the following equations,

$$\frac{u}{f}=\frac{U}{f-W} \qquad (1)$$
$$\frac{v}{f}=\frac{V}{f-W}.$$

This transformation is called the perspective transformation. For matrix-based handling, homogenous coordinates are often used. The object point with the world coordinate (U,V,W) is expressed by the homogeneous coordinate (kU,kV,kW,k). Here k is a nonzero arbitrary constant.

In the case that the world coordinate and the camera coordinate have a common origin and the common coordinate axes as shown in Fig.3, two dimensional camera image coordinate (*u*,*v*) is expressed by the world coordinate as $(u,v,w)=(u,v,0)$. Its homogeneous coordinates are defined as (ku,kv,kw,k). Then the perspective transformation is expressed by the following equation.

$$\begin{bmatrix} ku \\ kv \\ kw \\ k \end{bmatrix} = \begin{bmatrix} 1 & 0 & 0 & 0 \\ 0 & 1 & 0 & 0 \\ 0 & 0 & 0 & 0 \\ 0 & 0 & -1/f & 1 \end{bmatrix} \begin{bmatrix} U \\ V \\ W \\ 1 \end{bmatrix} \qquad (2)$$

Here, we put $k=1$.

In the imaging with the GC, due to the property of collimator, the relationship between an object point (*X*,*Y*,*Z*) and its image coordinate (*x*,*y*) can simply be expressed by the following equations,

$$x = X \qquad (3)$$
$$y = Y$$

In this research, we assume that the object surface can be approximated by a plane parallel to xy-plane and its z axis component can be estimated by the laser projection method.

Two world coordinates, (X,Y,Z) and (U,V,W) are related each other by rotation and translation and expressed by the homogenous coordinate representation as

$$\begin{bmatrix} U \\ V \\ W \\ 1 \end{bmatrix} = \begin{bmatrix} T_{11} & T_{12} & T_{13} & T_{14} \\ T_{21} & T_{22} & T_{23} & T_{24} \\ T_{31} & T_{32} & T_{33} & T_{34} \\ 0 & 0 & 0 & 1 \end{bmatrix} \begin{bmatrix} X \\ Y \\ Z \\ 1 \end{bmatrix}. \quad (4)$$

Here $T_{ij}, i = 1 \cdots 3, j = 1 \cdots 4$ are the parameters determined by the rotation and translation.

Furthermore the world coordinate (U,V,W) is perspective-transformed by the OC as mentioned in Eq. (2). Total transformation is therefore given by the following equation.

$$\begin{bmatrix} ku \\ kv \\ kw \\ k \end{bmatrix} = \begin{bmatrix} 1 & 0 & 0 & 0 \\ 0 & 1 & 0 & 0 \\ 0 & 0 & 1 & 0 \\ 0 & 0 & 1/f & 1 \end{bmatrix} \begin{bmatrix} T_{11} & T_{12} & T_{13} & T_{14} \\ T_{21} & T_{22} & T_{23} & T_{24} \\ T_{31} & T_{32} & T_{33} & T_{34} \\ 0 & 0 & 0 & 1 \end{bmatrix} \begin{bmatrix} X \\ Y \\ Z \\ 1 \end{bmatrix} \quad (5)$$

Actually, in the OC image, it holds

$$kw = 0 \quad (6)$$

So, it is not necessary to consider the third row. We therefore remove the third row and re-express the above equation as follows,

$$\begin{bmatrix} ku \\ kv \\ k \end{bmatrix} = \begin{bmatrix} C_{11} & C_{12} & C_{13} & C_{14} \\ C_{21} & C_{22} & C_{23} & C_{24} \\ C_{31} & C_{32} & C_{33} & C_{34} \end{bmatrix} \begin{bmatrix} X \\ Y \\ Z \\ 1 \end{bmatrix} \quad (7)$$

The parameters *Cij* can be determined by a calibration. Once the each element *Cij* are determined and *Z* component in the right hand side is given by the laser projection method, *uv* coordinates are uniquely related to *XY* coordinates as follows.

Now let the *Z* component of the object point be $Z = Z_C$ so as to express explicitly that the value is known. Substituting *k* of the third row into the first and second rows, we have

$$\begin{aligned} (C_{31}X + C_{32}Y + C_{33}Z_C + C_{34})u &= C_{11}X + C_{12}Y + C_{13}Z_C + C_{14} \\ (C_{31}X + C_{32}Y + C_{33}Z_C + C_{34})v &= C_{21}X + C_{22}Y + C_{23}Z_C + C_{24} \end{aligned} \quad (8)$$

The above linear equation gives the relationship between the GC image coordinates (*x*,*y*) and the OC image coordinate (*u*,*v*).

Estimation of distance between camera and object is done as follows. The locus of laser light is expressed using the XYZ coordinate as

$$\frac{X - X_0}{a_x} = \frac{Y - Y_0}{a_y} = \frac{Z - Z_0}{a_z} \quad (9)$$

Here, (X_0, Y_0, Z_0) denotes a point that the laser light passes through and (a_x, a_y, a_z) denotes the direction of the light. Both are constant vectors. By removing Z, we have

$$X = \frac{a_x}{a_z}(Z - Z_0) + X_0, \quad Y = \frac{a_y}{a_z}(Z - Z_0) + Y_0. \quad (10)$$

For simplicity of representation, we express the above equations as

$$X = A_x Z + B_x, \quad Y = A_y Z + B_y. \quad (11)$$

Substituting X and Y into Eq. (7),

$$\begin{aligned} ku &= C_{11}(A_x Z + B_x) + C_{12}(A_y Z + B_y) + C_{13}Z + C_{14} \\ kv &= C_{21}(A_x Z + B_x) + C_{22}(A_y Z + B_y) + C_{23}Z + C_{24} \\ k &= C_{31}(A_x Z + B_x) + C_{32}(A_y Z + B_y) + C_{33}Z + C_{34} \end{aligned} \quad (12)$$

are obtained. Here, for example, substituting *k* of the third row into the first row,

$$\begin{aligned} &[C_{31}(A_x Z + B_x) + C_{32}(A_y Z + B_y) + C_{33}Z + C_{34}]u \\ &= C_{11}(A_x Z + B_x) + C_{12}(A_y Z + B_y) + C_{13}Z + C_{14} \end{aligned}. \quad (13)$$

is obtained. Solving this equation with respect to *Z* gives

$$Z = \frac{-(C_{31}B_x + C_{32}B_y C_{34})u + (C_{11}B_x + C_{12}B_y + C_{14})}{(C_{31}A_x + C_{32}A_y + C_{33})u - (C_{11}A_x + C_{12}A_y + C_{13})} \quad (14)$$

Terms inside the bracket are all constant and re-epxressing by D_1, D_2, D_3, D_4, a simple relationship between the image coordinate *u* and *Z* coordinate of the object point is obtained as

$$Z = \frac{D_1 u + D_2}{D_3 u + D_4}. \quad (15)$$

Similarly, a relationship between the image coordinate *v* and *Z* coordinate of the object point can be derived. It means that either value *u* or *v* is sufficient to estimate *Z*.

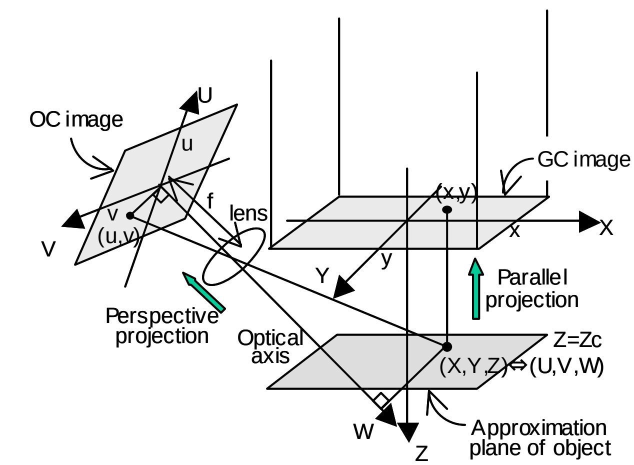

Fig. 3 Geometry and convention of coordinates of gamma camera imaging and optical camera imaging.

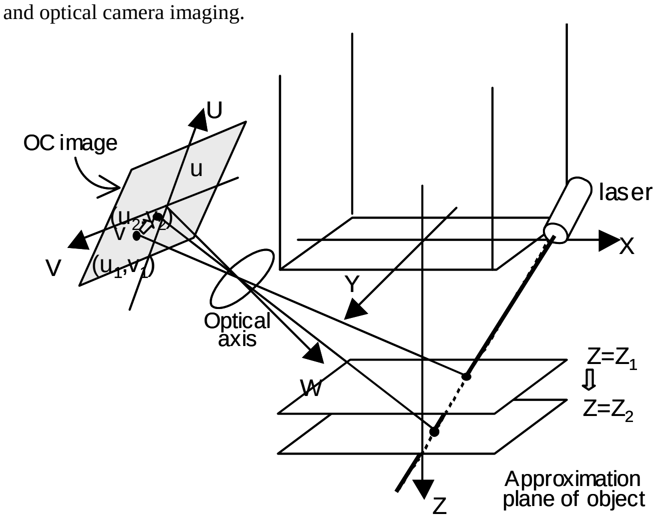

Fig. 4 Schematic illustration of estimation of the distance between the camera head and the object surface using a laser.

III. PRELIMINARY EXPERIMENT AND RESULTS

A. Setup

Fig. 5 (a) and (b) respectively show a picture of the setup used in the experiment and a picture around the GC head including GC, OC, LEDs and a diode laser. LEDs are used to illuminate the target in capturing optical images. The GC (MGC1500, Acrorad, Japan) utilizes semiconductor detectors, CdTe. The effective field of view the camera is 44.6mm x 44.6mm and is sampled by 32x32 channels. The pixel pitch is 1.4mm. The optical camera (Cyber eye, Japan) is a color CCD camera with about 410 thousand pixels and its viewing angle is about 120 degree. Laser module (H2-21, Audio-technica) is driven by DC 3V and emits 650nm light.

(a) the setup used in the experiment

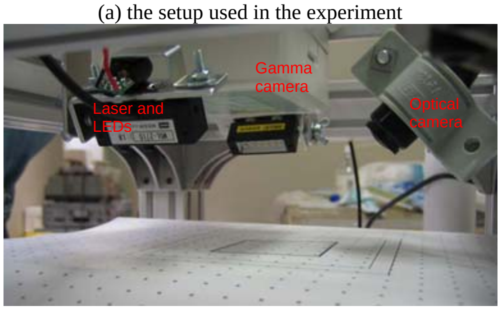

(b) a picture around the GC head

Fig. 4 Photos of the prototype setup.

B. Calibration

Before the use for image synthesis, three kinds of calibrations must be carried out as listed below.

(1) Calibration for distortion correction of OC image

(2) Calibration of distance estimation

(3) Calibration for mapping the OC image to GC image

The distortion of the OC is the camera's inner characteristics. Parameters for this calibration are obtained by capturing some straight lines and determining the parameters so as to straighten the lines curved by the distortion.

Calibration of distance estimation was carried out using a flat stage whose height (distance between camera and object) can be adjustable. Figure 6 shows the relationship between the v coordinate of Z coordinate. The open squares represent the measured data and the dotted line represents the model given by Eq. (15) fitted to the measured data. It shows that the distance estimation was successfully done.

It is noted that detection of the laser spot is performed automatically as follows. Two images are captured under laser on and laser off. Subtraction between two images is then calculated to enhance the laser spot. The center of the laser spot is easily detected from such an image. The sample images of this process are shown in Fig. 7.

In the calibration for mapping the OC image to GC image, several object points whose positions are known are captured by the GC. By applying the least square method to the set of pairs of image coordinates and world coordinates, the parameters *Cij* in Eq. (7) were obtained.

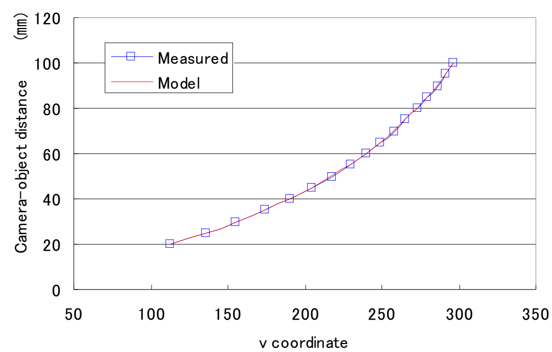

Fig. 6 Relationship between the v coordinate of Z coordinate. The open squares represent the measured data and the dotted line represents the model given by Eq. (15) fitted to the measured data.

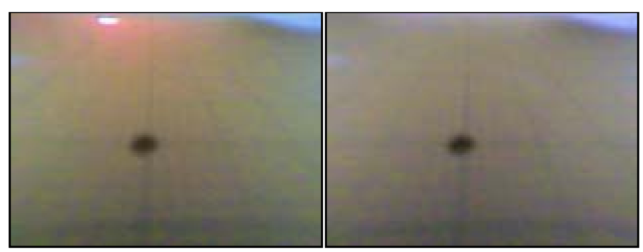

(a) Laser on (b) Laser ff

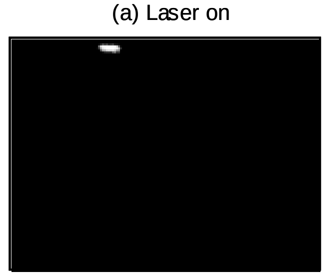

(c) Subtracted and binarized image

Fig. 7 Images with laser on and laser off and the subtracted and binarized image.

C. Synthesis experiment

Two preliminary experiments were carried out. In the first experiment, 99mTc, 0.1MBq was put at the end of syringe cap and used as tracer distribution. The tracer was put at several points below the GC and images were captured. Fig. 8(a) shows the original OC image when the tracer was put at the center of FOV of the GC. In this figure, the bold square drawn on the paper corresponds to the area just below the FOV of the GC. Fig. 8(b) shows the distortion corrected OC image. The lines are clearly straightened. Fig. 8(c) shows the GC image where high activities are observed around the center of the image. Finally Fig. 8(d) shows the synthesized image. In this image, the GC image is superposed onto the OC image by adding the red component of the color image. It is observed that the radioactivity well match to the OC image.

In the second experiment, tracer was put in both a syringe cap and a resected stomach. Results are shown in Fig. 9. The image arrangement is the same as Fig. 8. Again it is observed that the radioactivity well match to the OC image.

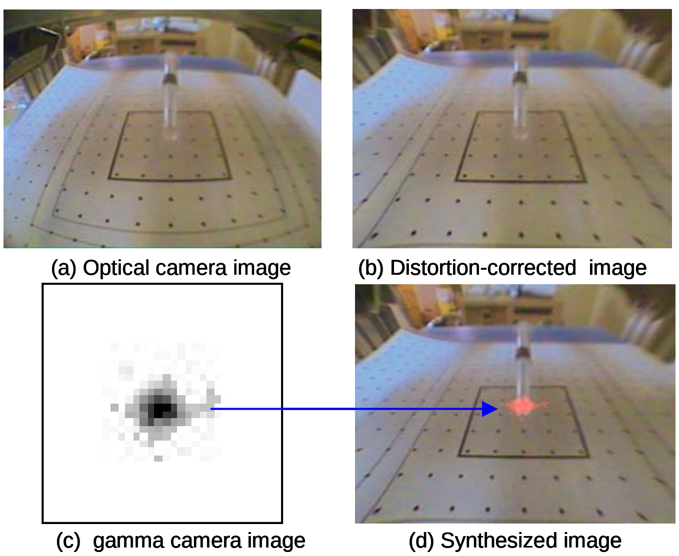

Fig. 8 Images obtained by the proto type setup. Tracer is put at the end of syringe cap. (a) Original OC image. Barrel distortion is observed. (b) Distortion-corrected image. Straight lines are corrected as straight lines. (c) GC output image. Tracer was put at the center of the viewing field (square) of GC. (d) Synthesized image. GC image is perspective-transformed and superposed onto the OC image as red image.

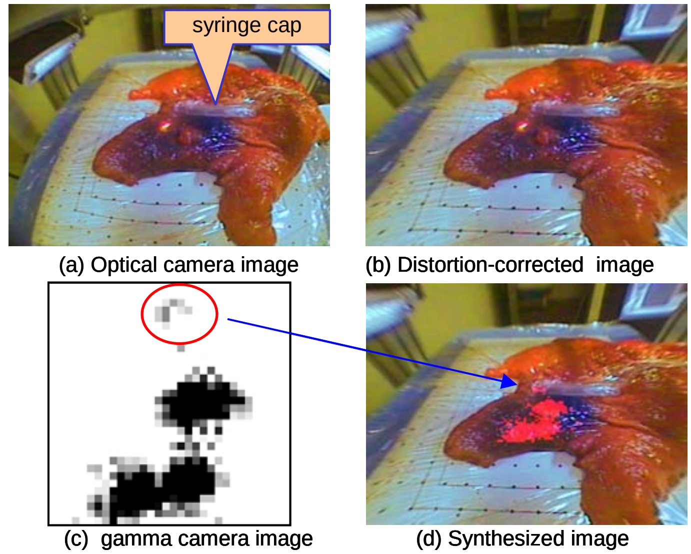

Fig. 9 Images obtained by the proto type setup. Tracer is put in both a syringe cap and a resected stomach. Image arrangement is the same as Fig. 8

IV. Conclusions

We have developed a method that combines a GC camera with an optical camera (OC) to synthesize two kinds of images and help surgeons to easily identify the SNs on the real surface. The method and preliminary experimental results with a prototype setup have been presented. We consider that the proposed method is applicable to the other application such as a small animal study and a breast cancer study.

V. References

[1] Hideki Hayashi, et al, “Sentinel Lymph Node Mapping for Gastric Cancer Using a Dual Procedure with Dye- and Gamma Probe-Guided Techniques”, J. American College of Surgeons, Vol. 196, No. 6, 2003, 68-74

[2] Makoto Tsuchimochi, et al, “A prototype small CdTe gamma camera for radioguided surgery and other imaging applications”, European Journal of Nuclear Medicine and Molecular Imaging Vol. 30, No. 12, December 2003

[3] Hideaki Haneishi, et al, “A new method for distortion correction of electronic endoscope images”, IEEE, Trans. on Medical Imaging, Vol. 14, No. 3, pp. 548-555 (1995)